Biblid: 1450-5029, (2025) 29; 2; p 37 - 42
DOI: 10.5937/jpea29-58258

Original Scientific Paper
Originalni naučni rad

HYDRODYNAMIC CAVITATION IN VENTURI CHANNELS WITH DIFFERENT DIVERGENT ANGLES
HIDRODINAMIČKA KAVITACIJA U VENTURI KANALIMA SA RAZLIČITIM DIVERGENTNIM UGLOVIMA

Ignacijo BILUŠ[1], Luka LEŠNIK[1], Luka KEVORKIJAN[1]*
[1]University of Maribor, Faculty of Mechanical Engineering, Maribor, Smetanova ulica 17, SI- 2000 Maribor, Slovenia
**Correspondence: ignacijo.bilus@um.si*

ABSTRACT

Hydrodynamic cavitation occurs in hydraulic systems when flow restrictions increase velocity and decrease pressure below vapor pressure. To study cavitation phenomena, simplified geometries such as Venturi channels are commonly used for experiments and numerical modeling. A Venturi channel gradually narrows to a throat before expanding at a diver gent angle, influencing cavitation characteristics. This study experimentally investigates the effect of divergent angles on cavitation formation and dynamics. Three 3D-printed inserts with different divergent angles were tested in a plexiglass cavitation tunnel. High-speed imaging (20,000 fps) with a Photron Fastcam SA-Z captured cavitation behavior, and an in-house Python script analyzed vapor projected area (a proxy for vapor volume) and cavity length. Results show that increasing the divergent angle reduces attached cavity length but produces larger detached cavitation clouds that travel farther before collapsing. The total cavitation projected area increased with larger divergent angles due to upstream movement of the cloud shedding point. These findings highlight the significant influence of divergent angle on cavitation behavior, with potential implications for cavitation-induced effects like erosion.

***Keywords**: cavitation, Venturi, high-speed video, cloud shedding, image postprocessing*

REZIME

Hidrodinamička kavitacija se javlja u hidrauličkim sistemima kada ograničenja u protoku povećavaju brzinu i smanjuju pritisak ispod pritiska isparenja. Za proučavanje pojava kavitacije često se koriste pojednostavljene geometrije poput Venturi kanala, kako u eksperimentima, tako i u numeričkom modeliranju. Venturi kanal se postepeno sužava do grla, a zatim širi pod divergentnim uglom, što utiče na karakteristike kavitacije. Ovo istraživanje eksperimentalno ispituje uticaj divergentnih uglova na formiranje i dinamiku kavitacije. Tri uložka izrađena 3D štampom sa različitim divergentnim uglovima testirana su u kavitanionom tunelu od pleksiglasa. Brzinska kamera Photron Fastcam SA-Z (20.000 fps) snimala je ponašanje kavitacije, dok je internim Python skriptom analizirana projektovana površina pare (kao pokazatelj zapremine pare) i dužina kavitacione šupljine. Rezultati pokazuju da povećanje divergentnog ugla smanjuje dužinu pričvršćene šupljine, ali proizvodi veće odvojene kavitacione oblake koji putuju dalje pre kolapsa. Ukupna projektovana površina kavitacije povećava se sa većim divergentnim uglovima usled pomeranja tačke odvajanja oblaka uzvodno. Ova otkrića naglašavaju značajan uticaj divergentnog ugla na ponašanje kavitacije, sa potencijalnim posledicama po efekte izazvane kavitacijom,poput erozije.

***Ključne reči**: kavitacija, Venturi, video velikih brzina, odvajanje oblaka, obrada slika*

INTRODUCTION

Cavitation is mass transfer phenomenon, where evaporation occurs due to a local drop of pressure in the liquid bellow vapor pressure. To differentiate cavitation from boiling, it is emphasized that this process occurs at constant temperature. When the pressure in the liquid rises back above the vapor pressure, condensation occurs, and previously formed vapor structures vanish in what is termed a vapor structure collapse or an implosion. Implosions of vapor structures produce secondary effects due to the release of pressure waves in the liquid. These secondary effects are often undesired, such as cavitation noise and cavitation erosion, which can occur when a pressure wave reaches a solid surface.

One particularly interesting topic of investigation is hydrodynamic cavitation, where the local drop in pressure is a consequence of the flow restriction, where velocity of the flow is locally increased, and pressure is decreased. This flow scenario can be found in many engineering applications, such as pumps, turbines, valves, ship propellers and other, many of which can be found in use in agriculture as well. When cavitation occurs in these engineering applications, there is a risk that secondary effects of cavitation can cause damage of the components and reduce the overall efficiency of a hydraulic system. Therefore, much of the research in cavitation has been focused on the topic of cavitation erosion, with a particular goal to develop numerical models that could be used within existing computational fluid dynamics (CFD) tools, to predict cavitation erosion of hydraulic systems. However, for development of cavitation erosion models, real hydraulic systems often prove to be too complex, either due to their size or due to the complexity of their geometry. To circumvent this obstacle, simpler geometries are preferred for research of cavitation and its effects. Use of this simpler geometry is also beneficial for the experimental work, either for validation of numerical models or as an independent research method. For internal flows Venturi channels are commonly used, the flow cross-section is restricted gradually in the channel as a nozzle with a convergent angle towards the minimum cross-section (throat), beyond which the cross-section gradually increases with a divergent angle.

Observation of cavitation (cavitation structures) is usually related to cavitation number, which is a single hydrodynamic parameter that describes the ratio of difference between reference static pressure and vapor pressure (p_v), and the reference dynamic pressure:

$$\sigma = \frac{p_{out} - p_v}{\frac{1}{2}\rho_l v_{th}^2}, \quad (1)$$

where the reference pressure is taken as the pressure at the outlet of the Venturi channel p_{out} and reference dynamic pressure for

liquid with density ρ_l is determined at the Venturi throat with reference velocity at the throat v_{th}. If the difference between reference static pressure and vapor pressure is fixed, the cavitation number varies with the flow rate (reference velocity) only. However, cavitation number alone does not describe how pressure distribution in the Venturi channel influences cavitation.

Dular et al. (*Dular et al., 2012*) experimentally investigated the effect of different dimensions on the dynamics of the re-entrant jet and in turn on the overall cavitation dynamics. They found that in the case of scaled-down Venturi test section the sheet cavity becomes stable to the point that cloud shedding was suppressed. Different shapes of the Venturi channel were considered in the numerical study by Saharan (*Kuldeep & Saharan, 2016*), where it was concluded that the shape of the channel influences the extent of cavitation as well as the intensity of collapses. Of particular interest was the divergent angle, for which it was found that the extent of cavitation was reduced at higher divergent angles, but intensity of collapses was increased. In the study by Li et al. (*Li et al., 2019*), influence of different parameters of Venturi channel for the generation of microbubbles were investigated both experimentally and numerically, where the influence of divergent angle on cavitation microbubble generation was observed. Detailed characterization of cavitation zone in various Venturis was done in the experimental and numerical study by Vijayan et al. (*Vijayan et al., 2023*), where it was found that the transition point of cavitation shedding mechanism moved away from the throat as the divergent angle increased. In a numerical study by Simpson and Ranade (*Simpson & Ranade, 2019*), divergent angle was identified as the most influential Venturi design parameter on cavitation extent and inception. Liu et al. (*Liu et al., 2020*) conducted the experimental study of the dynamic cavitation behavior in Venturis with various divergence angles and different cavitation numbers. They identified three distinct cavitation shedding regimes with respect to location of shedding initiation along the cavity length: front shedding, central shedding and tail shedding. For larger divergent angles shedding occurred more towards the front of the cavity, while for lower divergent angles it occurred more towards the tail of the cavity. Importance of Venturi divergent angle with respect to secondary effects has recently been highlighted in the study by Yang et al. (*Yang et al., 2025*), where cavitation erosion characteristics were investigated by way of experiment and Eulerian-Lagrangian numerical simulations. They observed that cavitation erosion risk was increased with a reduction in the divergent angle and the main erosion area was shifted downstream.

The need to investigate the influence of Venturi divergent angle on cavitation development is addressed in our study from the perspective of high-speed video observation of cavitation dynamics coupled with image postprocessing, which was also used in our previous investigation (*Kevorkijan et al., 2024*), to determine the cavity length. Additionally, cloud shedding is observed and is found to occur further upstream for larger divergent angles producing larger clouds which collapse further downstream.

MATERIAL AND METHOD

To study hydrodynamic cavitation in Venturi channels with different divergent angles, we conducted experiments in the cavitation tunnel at the Turbomachinery laboratory at the Faculty of Mechanical Engineering, University of Maribor. The cavitation tunnel, shown in Fig. 1, is a closed water loop. Through the closed loop, water is pumped with a centrifugal pump Lowara SHE 40-160/40 through the electromagnetic flow meter ABB WaterMaster FEV111, then it passes through a reservoir and into the straight pipe section which includes the plexi glass test section where cavitation is formed and observed and then returns towards the centrifugal pump through another reservoir.

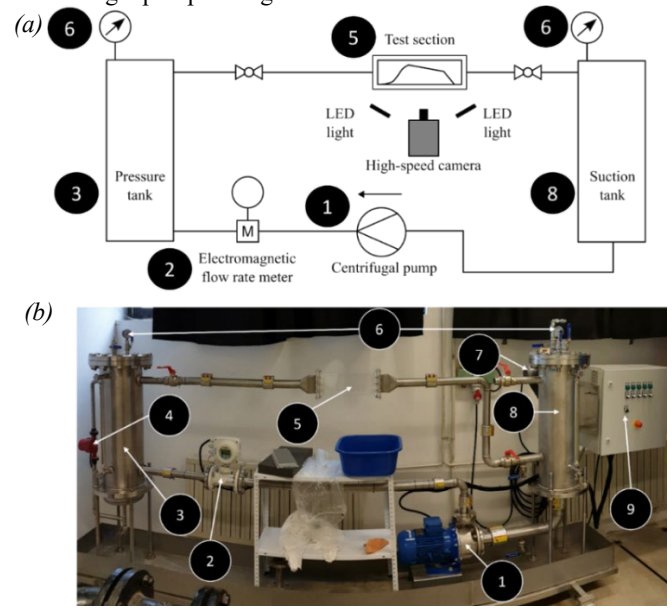

Fig. 1. Cavitation tunnel used in experimental work: (a) Schematics of the closed loop system; (b) Photograph of the cavitation tunnel in the laboratory. Several features of the cavitation tunnel are marked as: 1-centrifugal pump, 2- electromagnetic flow meter, 3-pressure tank, 4-additional tank recirculation pump, 5-plexi test section, 6-pressure gauges, 7-vacuum pump, 8-suction tank, 9-electrical controls.

To obtain the cavitation in the plexi test section, cross-section for the flow in the test section was reduced. This was achieved by using a 3D printed plastic insert, shaped to obtain a Venturi channel shape when inserted into the plexi glass test section, as shown in Fig. 2. In this study three different inserts were used, presented in Fig. 3. They differed in the divergent angle of the Venturi channel after the narrowing of the channel (throat). Thus, Venturi channels with a divergent angle of 4°, 8° and 12° were obtained and used in the experiments.

For each divergent angle of the Venturi channel experiments were conducted for three flow rates, therefore nine experiments were conducted. Pressure at the outlet of the Venturi channel (test section) was kept the same for all experiments. Then, per the definition of the cavitation number in Eqn. 1, cavitation number was only changed due to the change in flow rate, therefore for each divergent angle same three cavitation numbers describe the flow state, presented in detail in Table 1.

Table 1. Flow parameters for the three tested flow rates

Q [m^3/h]	v_{th} [m/s]	p_{in} [Pa]	p_{out} [Pa]	σ [-]
5.35	14.86	145,000	100,000	0.90
5.78	16.06	175,000	100,000	0.77
6.25	17.36	210,000	100,000	0.66

Hydrodynamic cavitation in each of the nine experiments was filmed with a high-speed camera Photron Fastcam SA-Z, capable of filming at up to 1,000,000 frames per second (fps). In this study videos were filmed at 20,000 fps, at this frequency the resolution used was 1024x512 pixels. Filming at high fps requires intense lighting, due to the short time the shutter of the camera is open. Therefore, two GSV_G8_KIT GSVITEC Multiled LED lights were used, each providing light with the temperature of 6500 K and luminous flux of 12,000 lm. The setup of high-speed camera with two LED lights is shown in Figure 1 (a).

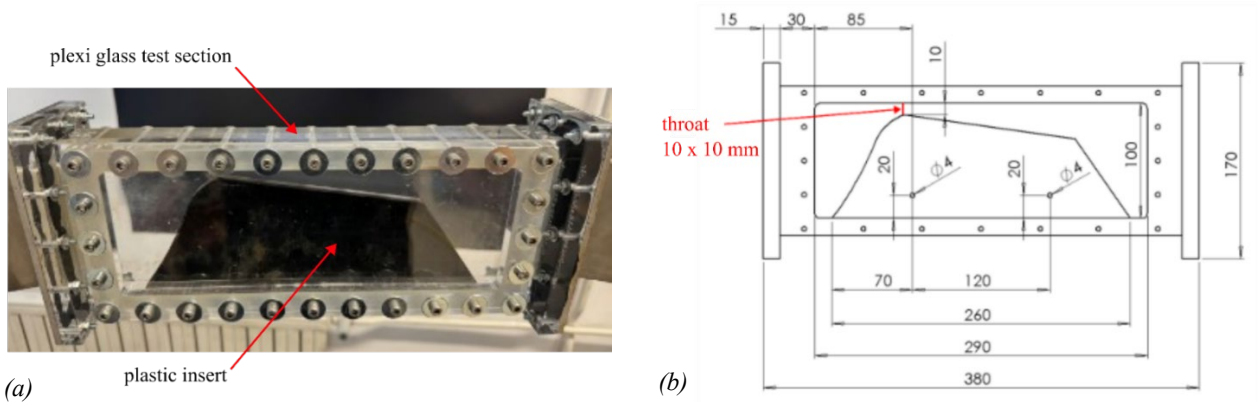

Fig. 2. Test section shaped into a Venturi channel: (a) Photograph of the plexi glass test section with inserted 3D printed plastic insert; (b) sketch of the test section including the plastic insert with dimensions indicated. Flow in the experiment is from left to right.

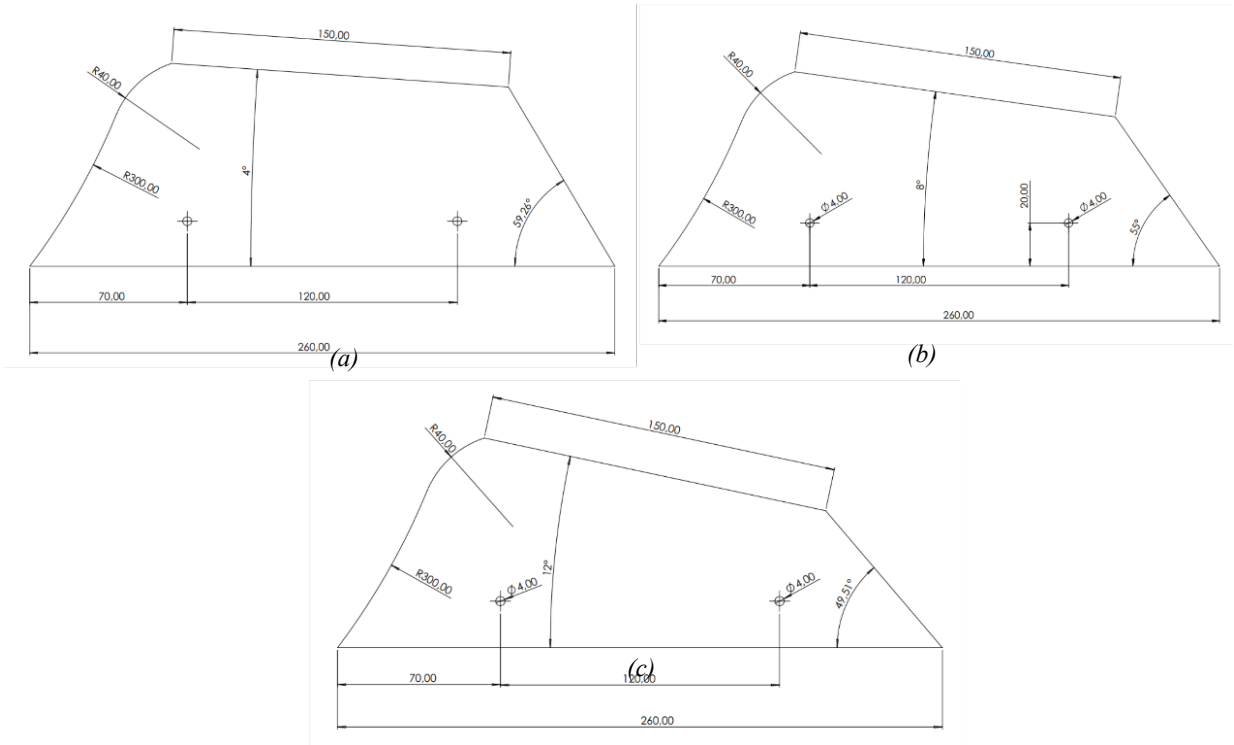

Fig. 3. Sketches of the three different inserts used in the experiments to obtain Venturi channels with three different divergent angles: (a) insert with the 4° divergent angle; (b) insert with the 8° divergent angle; (c) insert with the 12° divergent angle.

Many advanced flow visualization techniques exist, particularly for observation of shock waves *(Kozomora et al., 2024)*. Since we were interested only in macroscopic observation of cavitation structures, we decided to use standard high-speed video observation method. Rather, a more advanced postprocessing of the videos, broken down into series of images, was used to obtain more information. An in-house Python script based on the Open Computer Vision Library (OpenCV library) (*Bradski, 2000*) was used to convert a video file (mp4) into a series of images (png files). Then each image was cropped to desired dimension and converted from color to grayscale. Since the flow of clear water is transparent, a black background (black paper) was used when filming cavitation to have the flow of water represented with black pixels. Cavitation structures consist of vapor bubbles. The incoming light is reflected at the vapor-liquid interface of the bubble, therefore cavitation is seen as white on the images and white pixels therefore represent vapor. Pixels of the grayscale images were then filtered based on a previously determined threshold (between 0 and 255) (*Kevorkijan et al., 2024*) and assigned a value of 0 (black) or 255 (white), thus a binary, black and white image was obtained. Around connected white pixels, surrounded by black pixels, contours were drawn, using an algorithm proposed by (*Suzuki & Be, 1985*) and implemented in the OpenCV library (*Bradski, 2000*). According to the Green theorem, area inside the contour can then be calculated. This procedure was repeated for every image in a series of images, thus a total cavitation pixels area over time sampled in the high-speed video can be determined.

Finally, from the series of images, a composite image was created, where an average of all the pixels at a given position in the image was calculated to obtain a time-averaged image.

RESULTS AND DISCUSSION

First, we present the results for the 4° divergent angle, as shown in Figure 4, where initially at low flow rate (σ = 0.90) the vapor cavity is stable, and no shedding is observed.

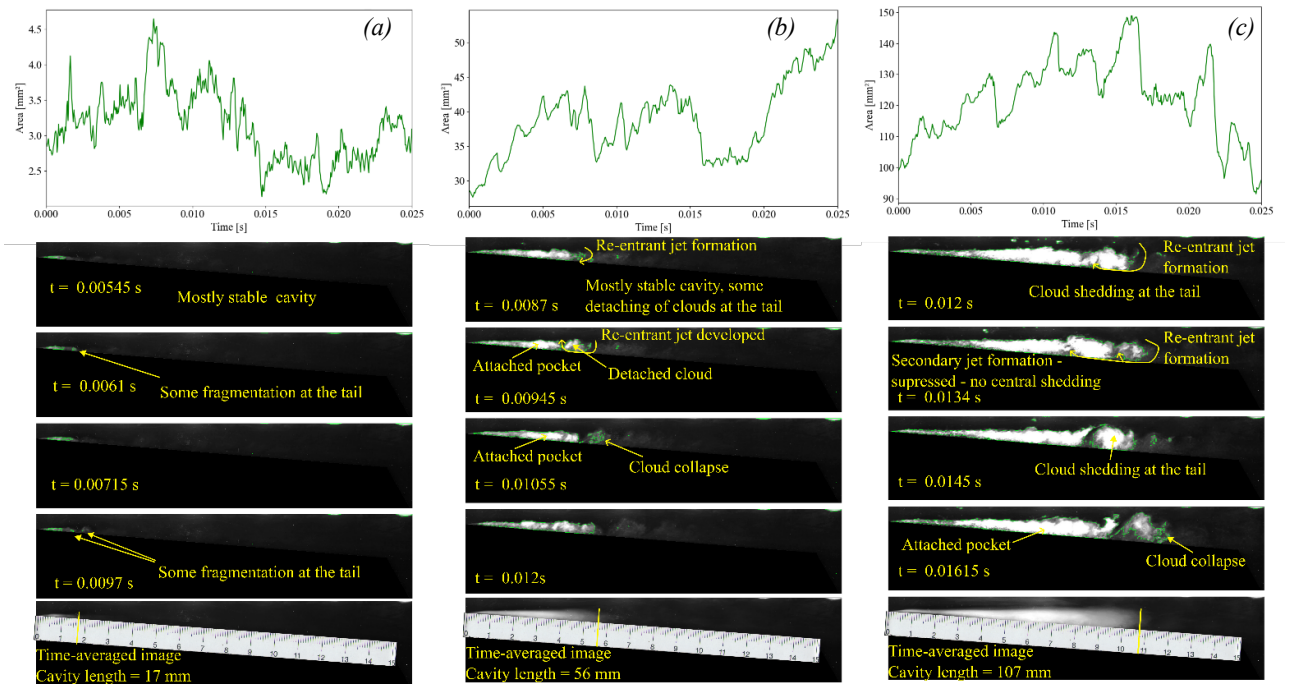

Fig. 4. Results for the Venturi channel with the 4° divergent angle: (a) flow rate of 5.35 m³/h and cavitation number of 0.90; (b) flow rate of 5.78 m³/h and cavitation number of 0.77; (c) flow rate of 6.25 m³/h and cavitation number of 0.66.

As the flow rate increases (cavitation number decreases), the extent of cavitation increases, and shedding dynamics occurs at the tail of the attached cavity. This shedding dynamics is the result of re-entrant jet formation, which curls around the tail of the cavity and turns back upstream underneath the cavity until a cloud separates and travels downstream. The increased extent of cavitation as the cavitation number decreases can be observed from the charts showing the calculated area of cavitation structures projected onto the camera lens. From the time-averaged images we can also measure the length of attached cavity, which is also observed to increase with decreasing cavitation number.

Similar tail shedding dynamics is observed in the case of the Venturi channel with the 8° divergent angle, presented in Figure 5. However, as the flow rate increases (cavitation number decreases), the cloud separation point moves towards the middle of the cavity and the re-entrant jet is less pronounced. From high-speed videos it is apparent that the collapse of a cloud from previous shedding cycle is concurrent with the reduction of attached cavity (a clear collapse front moving upstream through the attached cavity can be observed), which indicates the presence of a pressure wave propagating upstream. Again, the extent of cavitation increases with decreasing cavitation number.

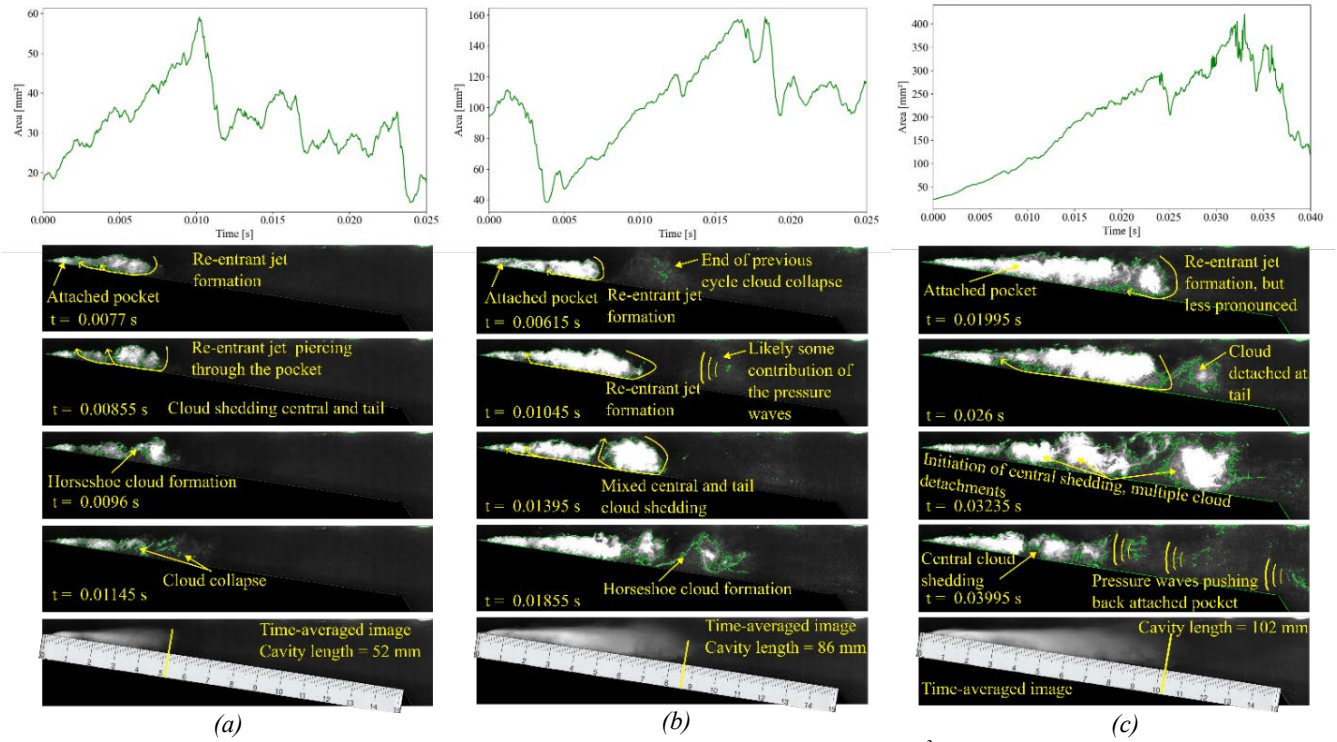

(a) *(b)* *(c)*

Fig 5. Results for the Venturi channel with the 8° divergent angle: (a) flow rate of 5.35 m³/h and cavitation number of 0.90; (b) flow rate of 5.78 m³/h and cavitation number of 0.77; (c) flow rate of 6.25 m³/h and cavitation number of 0.66.

For the Venturi channel with the 12° divergent angle, some tail shedding alongside central shedding is again observed for the case where the cavitation number was 0.90 (low flow rate), as shown in Figure 6. As the flow rate increases, the point of cloud separation moves further upstream, in the case of high flow rate (cavitation number of 0.66), high degree of frontal cloud shedding is observed as the separation point moves towards the throat of the Venturi channel. As the shedding point moves towards the front of the cavity, a clearer initiation of shedding due to pressure wave from previous cloud collapse, is also observed.

When comparing all the results, we find that the extent of cavitation is influenced both by the cavitation number and the divergent angle of the Venturi channel. As the divergent angle increases, and cavitation number decreases larger area of cavitation is observed. Since cavitation is a three-dimensional phenomenon, we infer from two dimensional images, that a larger volume of vapor or volume of cavitation structures is present as well.

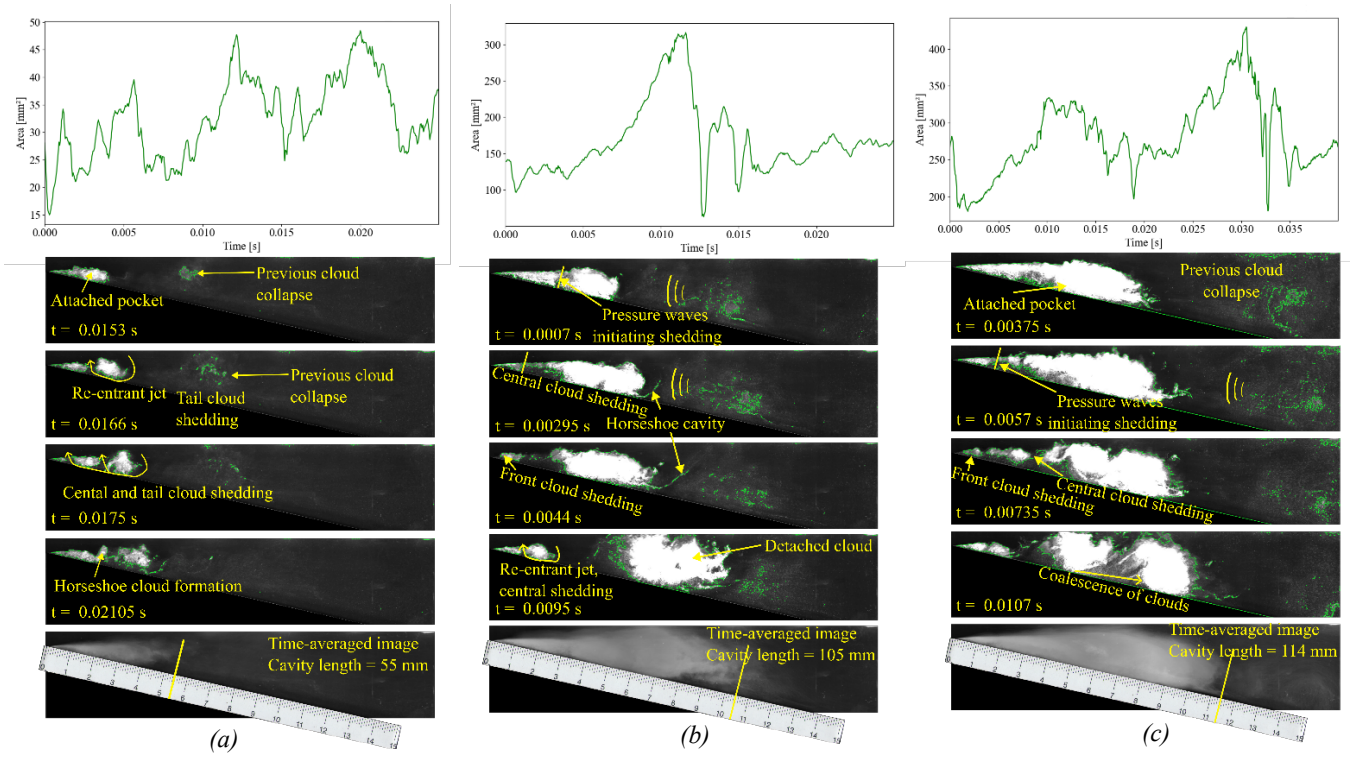

Fig. 6. Results for the Venturi channel with the 12° divergent angle: (a) flow rate of 5.35 m^3/h and cavitation number of 0.90; (b) flow rate of 5.78 m^3/h and cavitation number of 0.77; (c) flow rate of 6.25 m^3/h and cavitation number of 0.66.

Another way of observing the extent of cavitation is via the cavity length, which follows the same trend, as the divergent angle increases and cavitation number decreases, longer cavity is observed as presented in Table 2.

Table 2. Results of cavitation pocket length with respect to cavitation number and Venturi divergent angle.

Parameter		Divergent angle of the Venturi channel [°]		
		4	8	12
Cavitation number [-]	0.90	17 mm	52 mm	55 mm
	0.77	56 mm	86 mm	105 mm
	0.66	107 mm	102 mm	114 mm

The shedding dynamics, characterized by the position along the attached cavity at which clouds detach, is also influenced by both the cavitation number and the Venturi divergent angle. However, the Venturi divergent angle appears to play a more significant role, particularly at lower cavitation numbers, where shedding position clearly moves from tail to front as the divergent angle increases, as presented in Table 3.

Table 3. Results of cavitation cloud shedding type (by position) with respect to cavitation number and Venturi divergent angle.

Parameter		Divergent angle of the Venturi channel [°]		
		4	8	12
Cavitation number [-]	0.90	Stable cavity	Central/Tail shedding	Central/Tail shedding
	0.77	Tail shedding	Central/Tail shedding	Front/Central shedding
	0.66	Tail shedding	Central shedding	Front/Central shedding

CONCLUSION

Experimental study to determine the effect of Venturi channel divergent angle on the extent of cavitation and shedding dynamics was conducted by way of high-speed imaging coupled with image postprocessing. From the presented images, showcasing the cavitation shedding cycle for the 4°, 8° and 12° divergent angle and at different cavitation numbers, we concluded that alongside the cavitation number, the divergent angle has an impact on the extent of cavitation. At lower cavitation numbers there was more vapor present, which we evaluated via the projected area and the length of the attached cavity (obtained as a time-averaged image of cavitation).

Shedding dynamics was found to be dependent on the Venturi divergent angle as well. A clear shift from tail shedding to front shedding has occurred as the divergent angle increased. We associate this shift with a change in the underlying shedding mechanism, as suggested in the literature (*Liu et al., 2020).*

These findings highlight the importance of the flow geometry alongside the hydrodynamic parameters, especially as the flow state is described with a relatively robust quantity – the cavitation number, which does not account for all influencing parameters. This could further influence the secondary cavitation effects, for example cavitation erosion. By considering geometry parameters, cavitation erosion could be better mitigated in engineering applications used in agriculture.

ACKNOWLEDGMENT*: This work was supported by the Slovenian Research Agency (ARIS) in the framework of Research Program P2-0196 in Power, Process, and Environmental Engineering.*

REFERENCES

Bradski, G. (2000). The OpenCV Library. Dr. Dobb's Journal of Software Tools.

Dular, M., Khlifa, I., Fuzier, S., Adama Maiga, M., & Coutier-Delgosha, O. (2012). Scale effect on unsteady cloud cavitation.

Experiments in Fluids, 53(5), 1233–1250. https://doi.org/10.1007/s00348-012-1356-7

Kevorkijan, L., Paulin, M., Mauko, A., & Yılmaz, Y. E. (2024). Analiza hidrodinamične kavitacije v Venturijevem kanalu na podlagi

posnetkov hitre kamere pri različnih postavitvah osvetlitve.

Kozomora, V., Živkov, A., Vukić, M., & Oluški, N. (2024). Application of flow visualization methods for determining drag force

around a projectile. Journal on Processing and Energy in Agriculture, 28(1), 31–37. https://doi.org/10.5937/jpea28-49495

Kuldeep, & Saharan, V. K. (2016). Computational study of different venturi and orifice type hydrodynamic cavitating devices.

Journal of Hydrodynamics, 28(2), 293–305. https://doi.org/10.1016/S1001-6058(16)60631-5

Li, M., Bussonnière, A., Bronson, M., Xu, Z., & Liu, Q. (2019). Study of Venturi tube geometry on the hydrodynamic cavitation for the

generation of microbubbles. Minerals Engineering, 132, 268–274. https://doi.org/10.1016/j.mineng.2018.11.001

Liu, Y., Fan, H., Wu, D., Chen, H., Feng, K., Zhao, C., & Wu, D. (2020). Experimental investigation of the dynamic cavitation

behavior and wall static pressure characteristics through convergence-divergence venturis with various divergence angles. Scientific Reports, 10(1), 14172. https://doi.org/10.1038/s41598-020-68317-3

Simpson, A., & Ranade, V. V. (2019). Modeling hydrodynamic cavitation in venturi: Influence of venturi configuration on inception

and extent of cavitation. AIChE Journal, 65(1), 421–433. https://doi.org/10.1002/aic.16411

Suzuki, S., & Be, K. (1985). Topological structural analysis of digitized binary images by border following. Computer Vision,

Graphics, and Image Processing, 30(1), 32–46. https://doi.org/10.1016/0734-189X(85)90016-7

Vijayan, A., Kumar P., P., & Iyer, K. (2023). Experimental study and numerical sizing model for cavitation zone characterisation in cavitating venturis. Sādhanā, 48(2), 82. https://doi.org/10.1007/s12046-023-02131-1

Yang, Q., Chen, M., Pei, C., Liu, B., Zhao, M., Wang, X., Lin, Z., & Li, L. (2025). Experimental and Eulerian-Lagrangian numerical

investigation on cavitation erosion characteristics in Venturi pipes with different divergent angles. Ultrasonics

Sonochemistry, 114, 107278. https://doi.org/10.1016/j.ultsonch.2025.107278

Received: 17.03.2025. Accepted: 23.05.2025.